Controlling the hydraulic resistance of membrane biofilms by engineering biofilm physical structure

Desmond, Peter; Huisman, Kees Theo; Sanawar, Huma; Farhat, Nadia M.; Traber, Jacqueline; Fridjonsson, Einar O.; Johns, Michael L.; Flemming, Hans Curt; Picioreanu, Cristian; Vrouwenvelder, Johannes S.

DOI
10.1016/j.watres.2021.118031

Publication date
2022

Document Version
Final published version

Published in
Water Research

Water Research 210 (2022) 118031

Contents lists available at ScienceDirect

Water Research

journal homepage: www.elsevier.com/locate/watres

Controlling the hydraulic resistance of membrane biofilms by engineering biofilm physical structure☆

Peter Desmond [a,*], Kees Theo Huisman [b], Huma Sanawar [b], Nadia M. Farhat [b], Jacqueline Traber [c], Einar O. Fridjonsson [d], Michael L. Johns [d], Hans-Curt Flemming [e,f,g], Cristian Picioreanu [b], Johannes S. Vrouwenvelder [b,h]

[a] Institute of Environmental Engineering, RWTH Aachen University, Mies-van-der-Rohe-Strasse 1, D52074 Aachen, Germany
[b] Biological and Environmental Sciences and Engineering Division, Water Desalination and Reuse Center King Abdullah University of Science and Technology, Thuwal 23955-6900, Saudi Arabia
[c] Department of Process Engineering, Swiss Federal Institute for Aquatic Science and Technology (EAWAG), Dübendorf 8600, Switzerland
[d] Department of Chemical Engineering, The University of Western Australia, Crawley, WA 6009, Australia
[e] Singapore Centre for Environmental Life Sciences Engineering (SCELSE), 60 Nanyang Drive, 637551, Singapore
[f] Biofilm Centre, Faculty of Chemistry, University of Duisburg-Essen, Universitätsstr. 5, 45141, Essen, Germany
[g] IWW Water Centre, Moritzstrasse 26, 45476, Muelheim, Germany
[h] Department of Biotechnology, Faculty of Applied Sciences, Delft University of Technology, Van der Maasweg 9, 2629 HZ, Delft, Netherlands

ARTICLE INFO

Keywords:
Biofilm
Hydraulic resistance
Membrane filtration
Physical structure
Density

ABSTRACT

The application of membrane technology for water treatment and reuse is hampered by the development of a microbial biofilm. Biofilm growth in micro-and ultrafiltration (MF/UF) membrane modules, on both the membrane surface and feed spacer, can form a secondary membrane and exert resistance to permeation and crossflow, increasing energy demand and decreasing permeate quantity and quality. In recent years, exhaustive efforts were made to understand the chemical, structural and hydraulic characteristics of membrane biofilms. In this review, we critically assess which specific structural features of membrane biofilms exert resistance to forced water passage in MF/UF membranes systems applied to water and wastewater treatment, and how biofilm physical structure can be engineered by process operation to impose less hydraulic resistance ("below-the-pain threshold"). Counter-intuitively, biofilms with greater thickness do not always cause a higher hydraulic resistance than thinner biofilms. Dense biofilms, however, had consistently higher hydraulic resistances compared to less dense biofilms. The mechanism by which density exerts hydraulic resistance is reported in the literature to be dependant on the biofilms' internal packing structure and EPS chemical composition (e.g., porosity, polymer concentration). Current reports of internal porosity in membrane biofilms are not supported by adequate experimental evidence or by a reliable methodology, limiting a unified understanding of biofilm internal structure. Identifying the dependency of hydraulic resistance on biofilm density invites efforts to control the hydraulic resistance of membrane biofilms by engineering internal biofilm structure. Regulation of biofilm internal structure is possible by alteration of key determinants such as feed water nutrient composition/concentration, hydraulic shear stress and resistance and can engineer biofilm structural development to decrease density and therein hydraulic resistance. Future efforts should seek to determine the extent to which the concept of "biofilm engineering" can be extended to other biofilm parameters such as mechanical stability and the implication for biofilm control/removal in engineered water systems (e.g., pipelines and/or, cooling towers) susceptible to biofouling.

☆ Submitted to Water Research.

* Corresponding author.
E-mail address: Desmond@isa.rwth-aachen.de (P. Desmond).

https://doi.org/10.1016/j.watres.2021.118031
Received 5 August 2021; Received in revised form 26 November 2021; Accepted 29 December 2021
Available online 2 January 2022

1. Introduction

Microbial biofilms derive their primary physical structure from extracellular polymeric substances (EPS) secreted by embedded bacteria at a phase boundary (e.g., solid/liquid) (Desmond et al., 2018c; Flemming et al., 2021). In engineering systems, such as membrane filtration, retention of microorganisms on the surface of the membrane and mass transfer of soluble substrate through the microbial layer and membrane barrier creates a favourable niche for biofilm growth (Flemming et al., 1996). The physical structure of a biofilm (e.g., porosity, density, mechanical properties) has more influence on the hydraulic resistance than either the mass of accumulated EPS or embedded microbial cells (Ding et al., 2016; Dreszer et al., 2013). The usual chronological order of biofilm affected membrane performance indicators are: first the feed channel pressure drop increase, followed by a permeate flux decline and, at a later stage, a salt passage increase (Siebdrath et al., 2019). The development of a biofilm on the membrane and feed spacer (called here "membrane biofilm") gives rise to a secondary barrier of biological nature, and, thus, can cause a decline in membrane process performance especially if biofilm permeability is lower than intrinsic membrane permeability ((McDonogh et al., 1994; Siebdrath et al., 2019). The hydraulic resistance of membrane biofilms exerts greatest impact on Microfiltration and Ultrafiltration membranes (MF/UF), with much less consequence for Nanofiltration and Reverse osmosis (NF/RO) membranes due higher intrinsic membrane resistance of the latter (Dreszer et al., 2013) (i.e., orders of magnitude greater than the hydraulic resistance of the membrane biofilm). RO biofilm development presents a greater problem for crossflow resistance (biofilm on spacers) and concentration polarisation (Bucs et al., 2015; Herzberg and Elimelech 2007; Siebdrath et al., 2019). The core of this review will deal with the biofilm effects on the hydraulic resistance of MF/UF membranes.

Biofilm development in MF/UF necessitates increasing the feed pressure to maintain water production and the need to apply chemical cleanings, and in ultimate cases untimely membrane replacement. Membrane cleaning and frequent membrane replacement represents a significant portion of operating expenditure (OPEX) and should be reduced to allow economic operation (Jafari et al., 2020; Vrouwenvelder et al., 1998).

Decades of research focussing on biofilm inactivation or biofilm dispersion by non-specific reagents (e.g., enzymes, surfactants, inorganic salts, pH-shifts) did not succeed in controlling microbial biofouling and reducing biofilm hydraulic resistance on a long term (Nguyen et al., 2012). In principle, all membrane systems in water treatment carry biofilms, but not all of them suffer from biofouling caused by the presence of a biofilm. Gravity driven membrane (GDM) filtration even benefits from the biofilm presence due to stable flux production and laboratory experiments reporting improvements in permeate quality (Chomiak et al., 2015). Even for GDM filtration, the permeate flux is rather low. Whether a system exhibits biofouling depends upon the extent of the contribution of biofilms to flux decline. This observation lead to the concept of the "threshold of interference (a.k.a. "pain threshold") above which biofilm effects meet arbitrary operational and "biofouling" is diagnosed while below this threshold, no "biofouling" is recorded Flemming (2020) (Fig. 1).

The realisation that membrane filters could maintain a reasonable hydraulic permeability without complete removal of the biofilm under continuous dead-end conditions, therein keeping biofilms below the "pain threshold" (Griebe and Flemming 1998), prompted fundamental investigations into factors determining the hydraulic resistance of membrane biofilms (Peter-Varbanets et al., 2010; Peter-Varbanets et al., 2011; Peter-Varbanets et al., 2009). Specific structural features of membrane biofilms were associated to biofilm hydraulic resistance (e.g., thickness, surface roughness, density stratification) (Chomiak et al., 2014; Desmond et al., 2018a; Desmond et al., 2018c; Jafari et al., 2018).

The identification of biofilm physical structures which imposed low hydraulic resistance during membrane filtration made plausible the possibility of engineering biofilms with a morphology below the threshold of interference for long term operation without membrane cleaning (Jafari et al., 2018; Javier et al., 2020a). Advancement was made in linking not just biofilm hydraulic resistance to specific physical

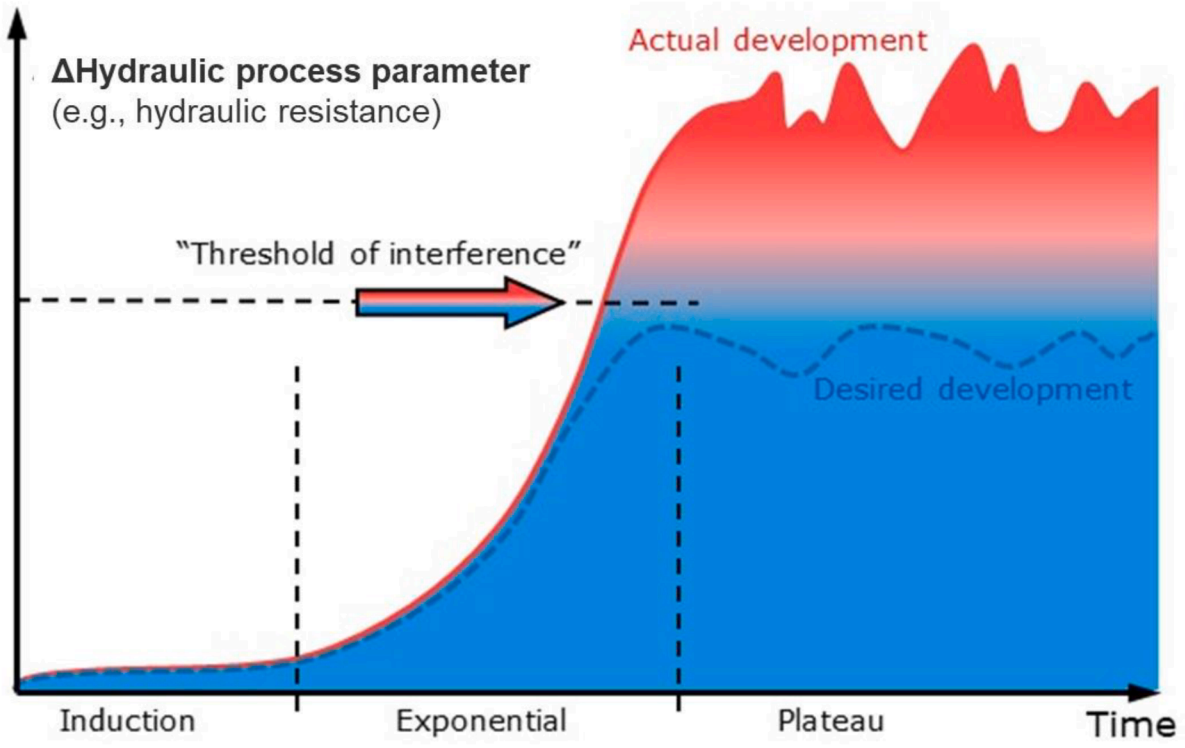

Fig. 1. Development of biofilms and the "Threshold of interference" above which biofouling is reported. The Δ(Parameter) represents the absolute change in any important hydraulic process parameter (e.g., hydraulic or friction resistance, pressure drop, permeate flux) due to the biofilm formation. While the actual process development exceeds the threshold (red curve), it is desired to keep the biofilm effects below this threshold of interference (adapted after Flemming (2011)).

structures, but also to the specific pre-treatment strategies (e.g., limitation of nutrients by granular activated carbon (GAC) filtration) and process operational conditions (e.g., Transmembrane pressure) required engineer biofilms below the "pain threshold" (Javier et al., 2020a; Javier et al., 2020b; Tang et al., 2016; Tang et al., 2018).

2. Linking hydraulic resistance to the physical structure of membrane biofilms

Total filtration resistance during MF/UF is defined by the resistance-in-series (RIS) model Foley (2013). The RIS model is widely employed to uncouple parameters influencing flux decline such that; $J = \frac{\Delta P}{\mu(R_m+R_{pb}+R_f)}$, where J is flux through the membrane (L/m^2/h), ΔP is the transmembrane pressure (bar), μ is the dynamic viscosity (Pa s), R_m is the membrane hydraulic resistance, R_{pb} is the pore blockage resistance and R_f is the fouling (biofilm/cake) resistance (all resistance are in m^{-1}).

Distinguishing to what extent one or more parameter (R_m, R_{pb}, R_f) governs overall filtration resistance is possible by comparing initial clean water flux and physical removal of the fouled membrane (Desmond et al., 2018a; Fortunato et al., 2016).

Studies reporting autopsy by physical scraping of the UF-biofilms, formed under various feedwater and process operational conditions, consistently evidenced the biofilm layer contributes ca. 60–80% to overall filtration resistance (Desmond et al., 2018a; Fortunato et al., 2016; Fortunato et al., 2017; Peter-Varbanets et al., 2010). Any "irreversible" increase in hydraulic resistance above the intrinsic resistance of the membrane after physical removal by scraping of the biofilm from the membrane surface is attributed to pore blockage (R_{pb}, 20–40%)) (Fortunato et al., 2016; Fortunato et al., 2017; Jermann et al., 2007). Pore-blocking may arise from adsorption of low molecular weight natural organic matter or biofilm-by-products (e.g., surfactants, biomass associated products (BAP)) into the membrane's pores. The lesser contribution of R_{bp} compared to R_f in UF membranes treating surface water may arise from the biofilm layer functioning as a secondary filtration barrier which can help reduce membrane adsorption and pore-blockage during filtration of natural organic matter (NOM) of polymeric and LMW acid range, as indicated for removal of viral particles (Heistad et al., 2009). Filtration resistance is additionally postulated to arise from adsorption (R_{ad}) of NOM to the membrane surface, and is considered as a recalcitrant fouling layer persisting after hydraulic removal of a "gel layer". However, in recent years, direct visualisation of the membrane surface revealed retention of a biofilm/gel residual layer of several micrometres that can resists hydraulic shear stress (Desmond et al., 2018b; Jafari et al., 2019) (Section 2.2). Thus, the historical consideration of R_{ad} may in fact be an indication of a residual biofilm layer, reflecting stratification in its cohesion and should be approached with caution in the absence of direct visualisation.

The dominant contribution of the surface biofilm (R_f) to overall filtration resistance supports the basis for dedicated efforts to engineer biofilms below the threshold of interference and is thus the focus of this review.

2.1. Hydraulics of biofilm layers

According to Darcy's law, $J = \frac{\kappa}{\eta}\frac{dp}{dz} J = \frac{\kappa}{\eta}\frac{dp}{dz}$, the flux of permeate J (i.e., volume passed per area filtration layer per time, m^3/m^2/s or L/m^2/h) is proportional with the pressure gradient (dp/dz) across the layer and the medium permeability κ, and inversely proportional with the passing fluid viscosity η (Seader et al., 1998). When the layer of thickness L is hydraulically homogeneous one can express Darcy's law also in terms of the specific resistance $R = L/\kappa$ (1/m) of that layer, as $J = \frac{\Delta p}{\eta R}$. When applied to a clean membrane, this becomes $J = \frac{p_f - p_p}{\eta R_m}$ with driving force being the pressure difference between the feed (p_f) and the permeate (p_p) sides of the membrane (Fig. 2A). With a biofilm fouling layer on the membrane surface, the biofilm resistance R_f adds in series with that of the membrane so that the decreased flux is $J = \frac{p_f - p_p}{\eta(R_m+R_f)}$, if the same pressure difference is maintained. Conversely, if operating at constant flux J, then the pressure difference must be proportionally increased to compensate the additional resistance, so that the transmembrane pressure (now $p_m - p_p$, Fig. 2B) remains the same. In general, both the membrane and the biofilm can comprise several sub-layers with different hydraulic properties, so that $J = \frac{p_f - p_p}{\eta\sum R_i}$. If one layer has a hydraulic resistance much larger than the others, that may determine the overall flux. For example, in RO the membrane resistance ($R_m \approx$

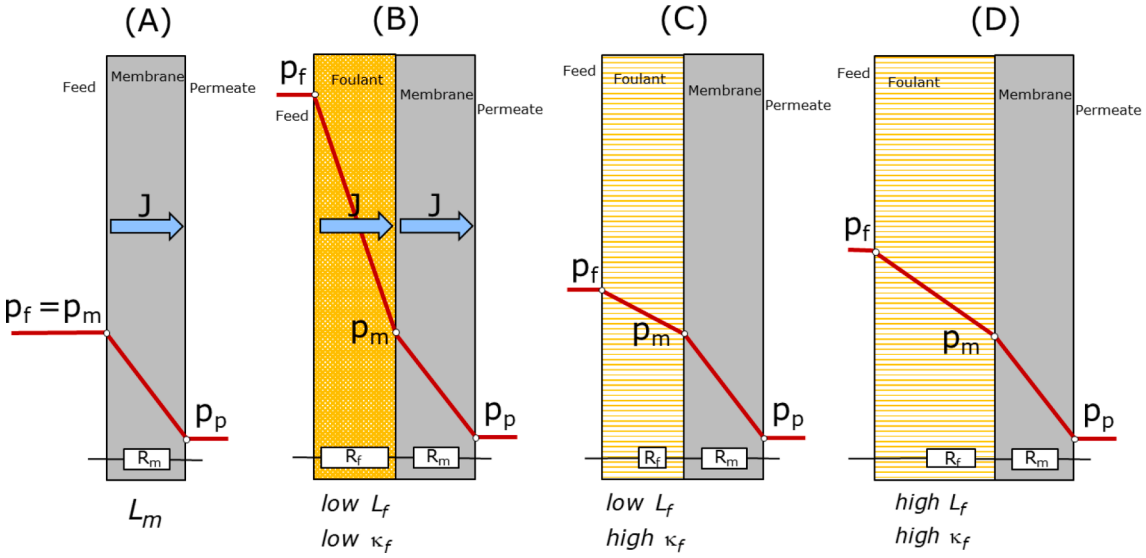

Fig. 2. Pressure difference needed when operating at constant permeate flux J: (A) in the absence of a biofilm layer; (B) with a rather impermeable (low κ_f) but thin biofilm layer; (C) with permeable (high κ_f) thin biofilm; (D) with permeable and thick biofilm layer. Note that the pressure difference across the membrane remains the same ($p_m - p_p$) driving the same flux J, while the overall pressure needed increases with $p_f - p_m$ to overcome the resistance of the biofilm layer. A continuity condition (equal fluxes) applies at the foulant/membrane interface, expressed as $J = \frac{p_f - p_m}{\eta R_f} = \frac{p_m - p_p}{\eta R_m}$. Graphic specifically illustrates the contribution of a biofilm layer as the most resistant layer during membrane ultrafiltration (60–80%), greater than the intrinsic resistance of the membrane (5–10%) and pore-blockage resistance (20–40%) (Desmond et al., 2018b; Fortunato et al., 2016; Jermann et al., 2007).

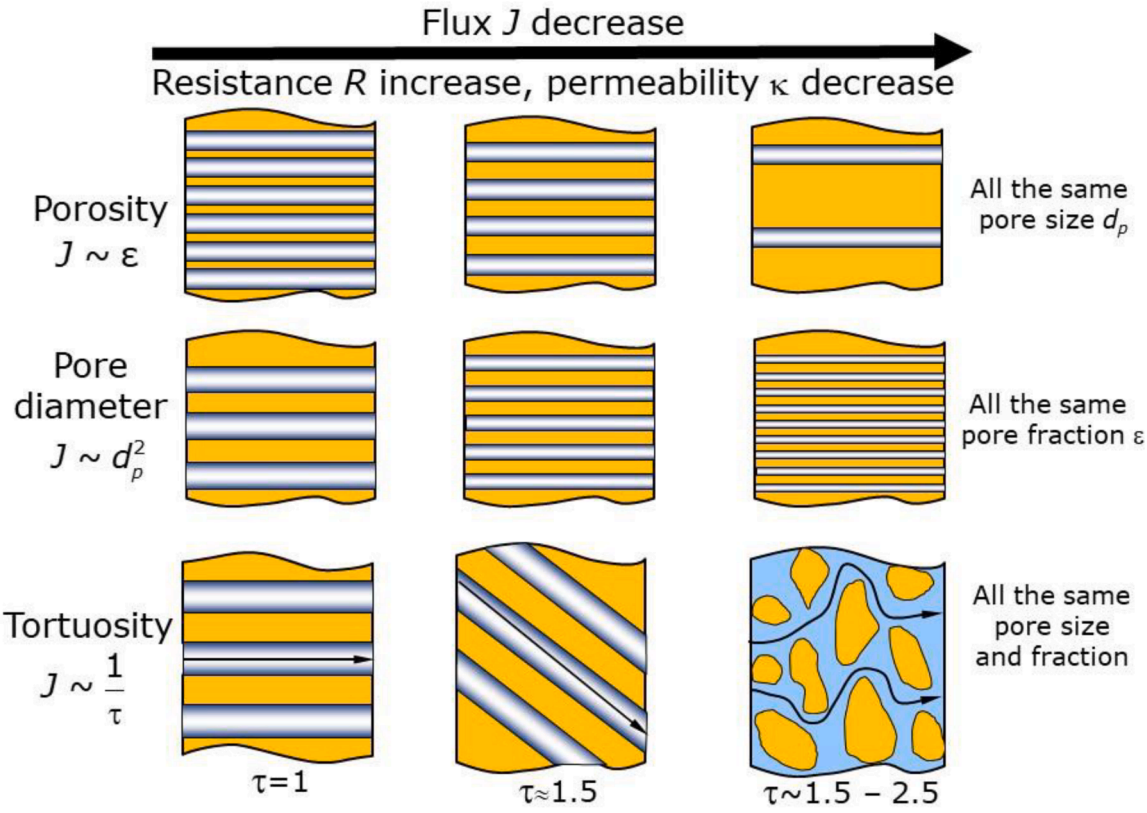

Fig. 3. The main factors influencing the permeability κ or resistance R of the biofilm layer are: porosity ε, pore size (diameter) and pore tortuosity (ratio between effective pore length and the shortest path possible). In addition, resistance R is an extensive measure increasing also with the layer thickness, L.

10^{16}–10^{17} 1/m, Radu et al. (2010)) dominates the biofilm resistance (R_f ≈10^{12} 1/m, Jafari et al. (2018)) by orders of magnitude, but in MF/UF ($R_m \approx 10^{11}$–10^{12} 1/m, Martin et al. (2014)) which makes the biofilm contribution very significant. Noticeably, not only the layer thickness L_f determines the characteristic resistance, but also its permeability κ_f, which implies that a thin but rather impermeable biofilm layer can reduce more the permeate flux (or requires increased pressure $p_f - p_p$ to drive the same flux) than a thick but permeable layer (Fig. 2C, D).

Several expressions for the hydraulic resistance of porous media have been derived, with the best known being: Hagen-Poiseuille $R_f = \frac{32}{d_p^2 \varepsilon} L_f$ assuming laminar flow through straight pores, Kozeny-Carman $R_f = \frac{180\tau}{d_p^2 \varepsilon^3/(1-\varepsilon)^2} L_f$ with inclined pores of tortuosity τ and Ergun $R_f = \frac{150}{d_p^2 \varepsilon^3/(1-\varepsilon)^2} L_f$ assuming packed spheres (Seader et al., 1998). All these relations acknowledge that the hydraulic resistance increases proportionally with an increase in the layer thickness L_f and pore tortuosity factor τ (which is the increase in effective hydraulic path compared with straight pores) and with the decrease of porosity ε, but strongly increases (quadratically) with a smaller pore diameter d_p (Fig. 3). Thus, larger (and more) pores can significantly increase the flux and decrease the hydraulic resistance compared to biofilm thickness alone.

Furthermore, in dynamic operation conditions (i.e., with changing transmembrane pressure TMP or permeate flux) the biofilms properties (L_f, ε, d_p, τ) can all be variable. Water permeation through the biofilm layer causes a structural rearrangement Casey (2007) with biofilm compression (Derlon et al., 2016; Desmond et al., 2018c) which decreases the porosity and increases the hydraulic resistance (Dreszer et al., 2014; Valladares Linares et al. 2015). As described by the mathematical model developed in Jafari et al. (2018) the extent of biofilm compression and subsequent hydraulic resistance increase results from the balance between forces due to permeate flow (i.e., pore pressure and permeate drag) and structural forces opposing deformation (i.e., biofilm viscoelasticity and plasticity). Gradients of porosity can develop within the biofilm layer (Jafari et al., 2019) along with gradients of mechanical strength which make compressed biofilms more difficult to be removed during the cleaning. These properties can be evaluated numerically with poroelasticity tools Coussy (2004) by coupling the fluid flow models through porous media (i.e., Darcy, Brinkman, etc.) with various solid mechanics models for the biofouling layer (i.e., elastic, elastoplastic, viscoelastic, etc.). When the numerical models are used in conjunction with microscopic (e.g., Optical Coherence Tomography (OCT)) measurements, values of the hydraulic parameters can be estimated, not only in simpler one-dimensional models of uniform thickness and homogeneous biofilm layer (Jafari et al., 2019), but also taking into account the effects irregular layer geometries (i.e. surface roughness) and heterogeneous or multiple layers (Jafari et al., 2019). An example of simulation results showing the dependency of flux on hydraulic and mechanical properties of heterogeneous biofilm layers is presented in Fig. 4.

2.2. Factors affecting biofouling layer hydraulic resistance

2.2.1. Biofilm thickness

For particle filtration, one commonly measures the particle mass deposited on the membrane surface m_f/A_m (kg/m^2) because it is related to the average cake layer thickness L_f and, therefore, it determines the filtration resistance. An increased mass per area is supposed to increase the passage length due to a thicker cake, leading to increased resistance when the particle volume fraction ϕ_s and density of solid particles ρ_s are constant and related by $m_f/A_m = \phi_s \rho_s L_f$ Foley (2013) and makes the broad assumption that the fouling layer is homogeneously distributed across the membrane surface.

Unlike a layer of inert particles, membrane biofilms are dynamic systems deviating from the expectation that mass accumulation is proportional to average thickness and thereof hydraulic resistance. Dreszer

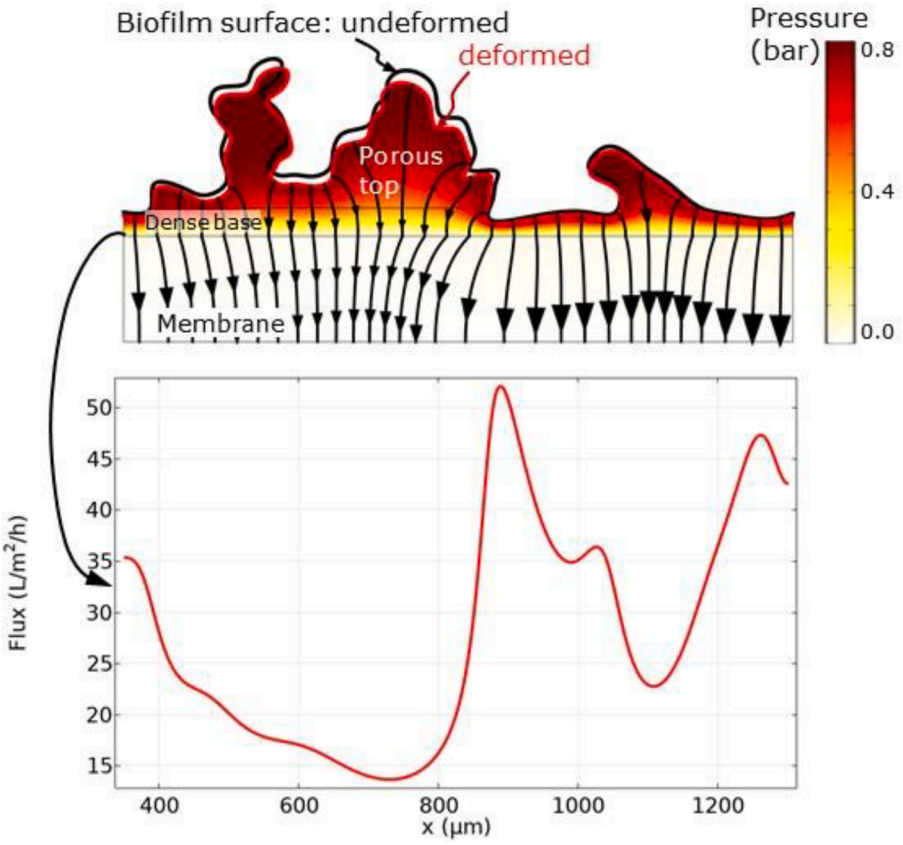

Fig. 4. An example of simulation of water flow through an irregularly-shaped and deformable biofilm on a membrane using the model from Jafari et al. (2019). (A) The main pressure drop is through the dense base of the fouling layer, while a relatively smaller pressure loss occurs in the top porous layer having variable thickness (roughness), both more important than the pressure loss through the membrane. (B) The water flux can be highly variable over the membrane length, with the largest values at positions of thinner fouling layer (as expected, at the lowest hydraulic resistance).

et al. (2013) used the relation between the measured mass accumulation and hydraulic resistance to determine an average biofilm thickness. When operating at a fixed permeate flux value of 20 L/m^2/h, resulting biofilms were thicker and with a higher permeability than biofilms formed under a permeate flux of 100 L/m^2/h. This suggested that thickness of the biofilm layer is not necessarily proportional to permeate flux or hydraulic resistance. Dreszer et al. (2013) concluded that the higher hydraulic resistance of the biofilm grown at 100 L/m^2/h was the effect of a higher density. A key limitation in the thickness calculation of Dreszer et al. (2013) is that the concentration of biofilm biomass is homogeneously distribution over the membrane surface. This however is not always the case and biofilm surface coverage is largely heterogeneously distributed across the membrane characterised by thick biomass "mounds" and "valleys" of thin biofilm (Derlon et al., 2012). Desmond et al. (2018a) later analysed biofilm structural morphology and average thickness by optical coherence tomography (OCT) and proposed that average biofilm thickness (thus the liquid passage length) can influence hydraulic resistance only in biofilms with a comparable morphology (e.g., biomass density/porosity and heterogeneity expressing the level of variability of these properties in space). On the other hand, significantly thicker biofilms (ca. 800 μm) with heterogenous morphology and lower density had lower hydraulic resistance compared to thinner biofilms (ca. 200 μm) with homogeneous morphology and higher density. It was determined that correlating hydraulic resistance to mean biofilm thickness was not accurate for heterogeneous biofilm structures and that other measures such as surface roughness (i.e. the heterogeneity of the biofilm thickness), in addition to density and pore fraction may play a significant role.

The use of OCT to measure average biofilm thickness is considered appropriate due to the high penetration depth allow high level of visualisation of both the biofilm-liquid interface and the biofilm-membrane interface. OCT is not restricted by incomplete biofilm-liquid interface visualisation due to potential for unstained constituents marring the use of fluorescence methods (Wagner and Horn 2017). While shadowing effects may occur, this is more so problematic for deriving internal biofilm architecture such as internal porosity but biofilm thickness (Derlon et al., 2012).

2.2.2. *Biofilm surface roughness*

Biofilm surface roughness is defined as the smoothness of the biofilm surface/liquid boundary layer as it relates to the variation in biofilm thickness (Wagner and Horn 2017; Wagner et al., 2010). Derlon et al. (2012) proposed the hydraulic resistance was influenced by biofilm surface roughness when comparing biofilm morphology and hydraulic resistance in gravity driven ultrafiltration systems with and without predation by higher organisms. The hydraulic resistance of thick "mounds" of biofilm interspersed by "valleys" of thin biofilm across the membrane surface, was postulated to be higher than biofilm adjacent to the membrane due to increased passage length (Derlon et al., 2012). Following a "line of least resistance", water was postulated to pass through the membrane where an absent or only a very thin biofilm is present (Derlon et al., 2012). Martin et al. (2014) provided a simulation-based description of the observations of Derlon et al. (2012). Biofilm layers with a high surface roughness (i.e. an irregular geometry) had lower hydraulic resistances compared to "flat" or compact fouling layers with a comparable thickness (Martin et al., 2014). For a given mean fouling layer thickness, an increase in spatial heterogeneity could increase the permeate flux by over an order of magnitude. The model results were dependant on several other factors, such as the membrane resistance, the fouling layer permeability, and EPS and cellular biomass spatial distribution.

Later Fortunato et al. (2017) studied the formation of surface roughness and the change of permeate flux during biofilm maturation. Contrary to the physical reality that the main flow should be directed through areas of low hydraulic resistance, their interpretation of computational fluid dynamic (CFD) simulations was that rough surface

appendages exhibited higher flux than the thinner structures (biofilm cavities) due to the presence of liquid vortices in the biofilm "valleys" which could lower the pressure gradient thus decreasing permeation. These results were contested by Jafari et al. (2019) who indicated that the small axial velocities would only lead to a negligible pressure drop compared to the trans-membrane pressure gradient, and that simulation results from Fortunato et al. (2017) were merely wrongly interpreted. Both Jafari et al. (2019) (see Fig. 4) and other CFD simulations with mass transfer (Radu et al., 2010; Radu et al., 2012) have also clearly shown how the higher flux (water passage) occurs through areas of thinner biofilm.

However, Desmond et al. (2018b) later demonstrated erosion of the rough biofilm surface layer (comprising ca. 60–80% overall biofilm thickness in biofilms formed on real and synthetic surface water) by incremental increases in hydraulic shear stress had a negligible impact on hydraulic resistance. This is comparable to observations in pilot and full-scale cross-flow ultrafiltration systems which report poor cleaning efficacy with hydraulic cleaning alone (Jafari et al., 2020). This also lends evidence to the suggestion that previously considered fouling mechanisms such as pore-blocking and adsorption may be attributed to a retained biofouling layer with high adhesion to the membrane. Morphological observations by OCT revealed retention of a residual densified biofilm (ca. 50–100 μm) with low surface roughness adjacent to the membrane (termed biofilm "base layer"). Physical removal of the base layer led to a reduction hydraulic resistance within 20% of the intrinsic resistance of the membrane, with the remaining hydraulic resistance accounted for by the intrinsic resistance (ca. 5%) of the membrane and pore-blockage (ca. 15%) (Fig. 5) (Desmond et al., 2018b). It was concluded the biofilm hydraulic resistance was governed by the biofilms base layer. The presence of a base layer was indicated by the stabilisation in biofilm thickness under increasing shear stress up to 3 Pa, observable at multiple positions along the flow-cell length (x-y coordinates) and is considered representative and valid structural feature of membrane biofilms. When compared to the conceptual model

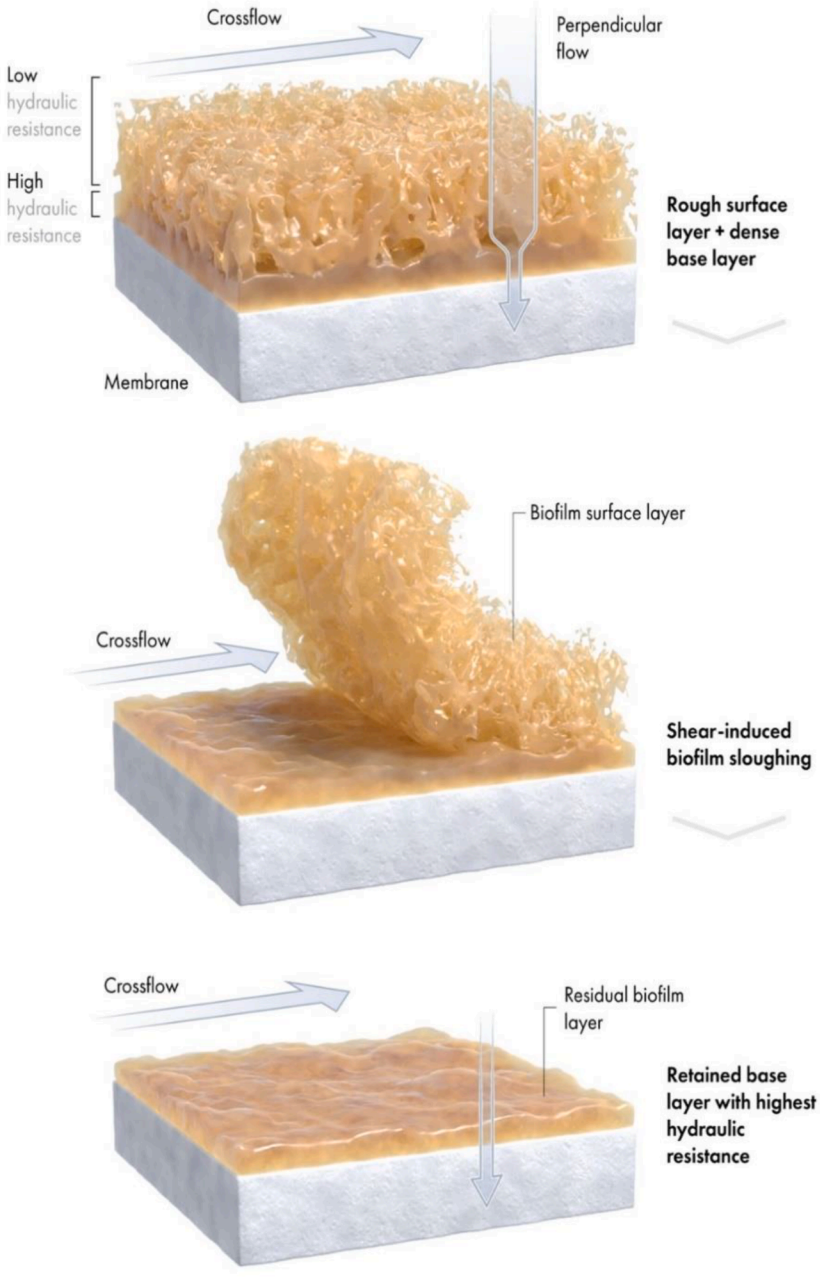

Fig. 5. Stratification in the physical structure of membrane biofilms reveals contribution of structural morphology on biofilm hydraulic resistance. Erosion of rough surface layer had limited impact on hydraulic resistance due to retention of a residual base layer which dominated overall hydraulic resistance. Illustrations based on actual biofilm dynamics formed on ultrafiltration membranes treating synthetic and real surface water, observed via continuous OCT imaging by Desmond et al. (2018b) and supported by numerical modelling of Jafari et al. (2019).

presented by Derlon et al. (2012), one could consider the "mounds" of biofilm to represent rough surface layer which exerts a lower hydraulic resistance compared to adjacent area of thin biofilm. However, stratification in biofilm hydraulic resistance and physical structure was not investigated by Derlon et al. (2012). Instead, authors broadly assumed the thickness exerted most amount of resistance as opposed to other structural parameters (e.g., density, porosity). Later numerical modelling by Jafari et al. (2019) demonstrated stratification in the hydraulic, structural and mechanical properties of membrane biofilms grown on similar feedwater (i.e., river water) to Derlon et al. (2012). This brought computational substantiation of the observations of stratification in hydraulic resistance reported by Desmond et al. (2018b).

2.2.3. Biofilm density

The density of the fouling layer proved to be a critical determinant of hydraulic resistance (Desmond et al., 2018a; Valladares Linares et al. 2015). The density of membrane biofilms, ρ_f (biofilm mass as kg total organic carbon (TOC) per m^3 biofilm), is empirically derived by the simple expression $\rho_f = m_f/(A_m L_f)$, where m_f is the biofilm mass (kg TOC), A_m is membrane surface area (m^2) and L_f is the average biofilm thickness (m) (Desmond et al., 2018a). More recently Fortunato et al. (2020) proposed biofilm density can be determined optically using OCT imaging by recording the ratio between the biomass pixels intensity and the background pixels intensity of a membrane biofilm. However, optical measurements were not validated by conventional density measurements, thereby limiting critical comparison to previous work. Moreover, quantitative analysis of internal biofilm structure using OCT imaging is oversimplified. Influent complexity (e.g., both soluble/non-soluble organic substrate), bulk suspended biomass and biofilm structure can reduce the certainty of whether visualized areas of low absent intensity are in fact areas of absent biomass or result from compositional (i.e., refractive index) heterogeneity, shadowing of overlying biomass and/or accumulated non-soluble substrate. Conclusions should not ultimately be drawn from quantified images without experimental controls that consider the role of experimental artefacts (e.g., particulate loading, shadowing from suspended biomass) which falsely present as areas of lower density and/or absent biomass.

Desmond et al. (2018a) compared the hydraulic resistance of biofilms with similar average thickness but different densities of calculated mass of extracellular polymeric substances and membrane area. Thin (ca. 100 μm) dense biofilms had a greater hydraulic resistance than thicker (ca. 800 μm) biofilms with lower EPS densities despite being several hundred micrometres thinner. EPS constitutes >90% of the biofilm's overall biomass concentration with a low fraction attributed to bacterial cell concentration (Desmond et al., 2018a; Dreszer et al., 2013). EPS density of membrane biofilms can be considered representative of the biofilm overall density. It was concluded that the EPS density and internal molecular packing density could impose greater resistance than biofilm thickness. Compacted biofilms (i.e. grown at a low pressure/flux, then exposed to higher pressures/fluxes) had an irreversible increase in hydraulic resistance. Valladares Linares et al. (2015) related the irreversible increase in hydraulic resistance to a corresponding increase in density (Fig. 6), namely, the same amount of biomass occupied a smaller microscale volume due to the reorganization of the biofilm, increasing the EPS concentration. Desmond et al. (2018c) calculated the biofilm density in gravity driven membrane systems and noted an increase upon compaction proportional to the observed increase in hydraulic resistance. This observation was supported by reversible compression and relaxation experiments on homogeneous biofilm structures. Further reversible compression/relaxation cycles caused a decrease in density and, thus, a reduction in hydraulic resistance. Thus, the changes in the EPS density (and not biofilm thickness) were suggested as the critical determinant for hydraulic resistance (Desmond et al., 2018a; Dreszer et al., 2013; Valladares Linares et al. 2015).

Biofilm density is also influenced by physical interactions (e.g. electrostatic) within the EPS (Mayer et al., 1999; Pfaff et al., 2021). Recently, Pfaff et al. (2021) found that by increasing the feedwater Ca^{2+}concentration the density of alginate fouling layer as well as its hydraulic resistance increased, and correlated to flux decline in membrane filtration. In their experiments the alginate layer density reached a plateau around 8 mM Ca^{2+} indicating saturation of anionic binding sides. It was hypothesised addition of Ca^{2+} created a salt bridge between two negatively charged residues via hydrogen bond formation (10–30 kJ/mol) to form an array of repeating polymeric blocks, termed an "egg box" configuration (Giraudier et al., 2004). Such interactions can form uniform packing structures with reduced volume between neighbouring strands of EPS leading to the formation of homogeneous biofilm physical structures. The hydraulic response of the alginate layer mirrored the hydraulic behaviour of polysaccharide fouling layers observed by Herzberg et al. (2009), albeit in reverse osmosis membrane systems. Herzberg et al. (2009) indicated calcium increases the adsorption of polysaccharides and DNA by 2- and 3-fold, respectively. The increased adsorption of EPS onto the membrane resulted in a significant decrease in permeate water flux, however the physical structure of the fouling layer was not quantified, limiting any link between a structural parameter and hydraulic resistance. The impact of EPS composition on biofilm physical structure and hydraulic resistance was later assessed by Desmond et al. (2018a) who substantiated the link between secretion of anionic EPS (polysaccharides and eDNA) increased density of actual biofilms, and not surrogate compounds, formed on ultrafiltration membranes under phosphorus limiting condition. The study of Desmond et al. (2018a) however made use of biofilms formed under synthetic raw water which lacked inclusion of complex nature organic matter and complex microbial community. Thus, the fidelity of biofilms formed under synthetic influent conditions, and also with surrogate compounds, compared to membrane biofilms is highly dubious. Simplified experimental models do not consider the complexity of natural organic matter/microecology and spatiotemporal variations present in more complex biofilm systems cultivated under environmental conditions (Jafari et al., 2020). This may account for the bias in literature towards reporting the detection and function of anionic as opposed

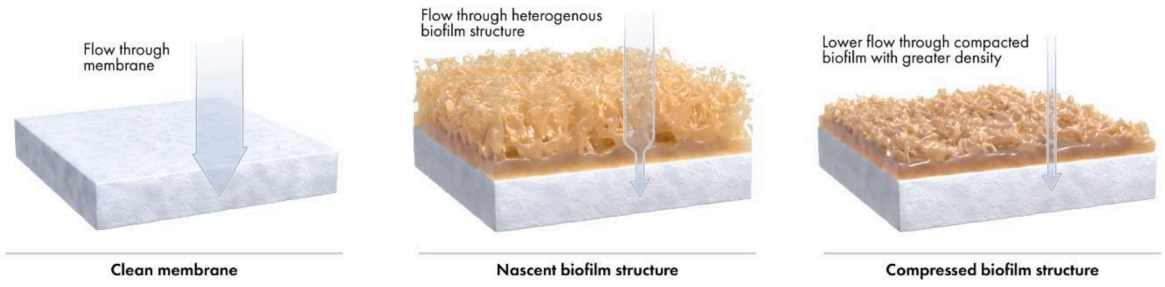

Fig. 6. Effect of biofilm compression. Increased permeate flux through the nascent structure of biofilms can lead to compaction of biomass on the membrane surface, resulting in a biofilm with greater density. Ultimately, the high-density biofilm will lower the permeate flow. Illustrations based on actual biofilm observations via OCT reported by Desmond et al. (2018c) and Valladares Linares et al. (2015).

to cationic and/or non-ionic polymers which may be preferentially selected in a simplified experimental system.

Despite the short-comings of typical experimental systems employed to study the hydraulic resistance of membrane biofilms, regardless of the specific system, the biofilm or surrogate layer with greater biopolymer density consistently exhibited a higher hydraulic resistance compared to less dense biofilms. The mechanism by which density affects hydraulic resistance is intuitively linked to the internal packing structure (e.g., porosity and polymer concentration per μm^3) which can be influenced by both mechanical stress and steric interaction between neighbouring polymeric strands. However, as discussed in the following section, the relationship between biofilm density and internal packing structure is difficult to delineate, with no formalized conceptual model or adequate methodological repertoire for examining the biofilm internal structure.

2.2.4. *Biofilm porosity*

The prevailing vista in biofilm literature is that biofilms exhibit discrete internal "pore-structures" in between construction material made of biopolymers (Fortunato et al., 2017; Melo 2005). The underlying assumption of this conceptual model is that the biofilm is a discontinuous structural matrix akin to "Swiss-cheese" (i.e., with holes) (Fig. 7A). Melo (2005) postulated biofilms exhibit a dual pore structure containing large macro-pores (water channels) interspersed by polymer aggregates and micro-pores inside these aggregates, as in models defining tortuosity for solute mass transfer. In the macro-pores, mass transfer of both water and solute could occur by both diffusion and convection. In smaller pores, water convection would face a high resistance due to greater packing density of EPS molecules and solute diffusion would prevail Melo (2005).

Later, application of OCT and CLSM with corresponding image analysis suggested initial evidence of pore-like structures at the biofilms meso- (>5 μm) and micro-scale (>0.2 μm) respectively (Fortunato et al., 2017; Peter-Varbanets et al., 2010). Fortunato et al. (2017) reported a decrease in porosity from quantified OCT images from 0.20 at day 5 to almost zero (where 0 is non-porous) corresponded with an increase in hydraulic resistance. Despite a near zero-porosity reading, water still permeated through the biofilm, indicating potential culverts below the axial resolution of the OCT (ca. 3 μm). While OCT has superior penetration, depth compared to CLSM, shadowing effects during OCT imaging might occur. This is problematic for reliable quantification of internal porosity from OCT images. Pore-like structures visualised using OCT are quantified as the number of void voxels in the biofilm layer. Analysis is performed on binarized data, whereas the pixels were classified in empty (0) and filled (1) (Wagner et al., 2010). The descriptor is the ratio of void space under the biofilm layer and the total biofilm area. However it is not possible to differentiate between areas of absent biomass and areas of low signal intensity arising from shadowing (Wagner and Horn 2017). Similar with the determination of biofilm density by OCT (Fortunato et al., 2017), correct experimental controls and/or complementary computation analysis is required when evaluating the biofilm porosity. Computational analysis by Jafari et al. (2018) indicated that hydraulic resistance is plausibly dependant on pore/particle reorganization but only at a scale lower than 3–5 μm, whereby when foulant layer deformation occurs below the detectable threshold (3 μm), biofilm hydraulic resistance would increase by 110%.

The computational work of Jafari et al. (2018) substantiated the earlier postulation from Peter-Varbanets et al. (2010) who reported the formation of microscale pore-like structures in biofilm layers in gravity driven ultrafiltration membranes using CLSM and an aquatic fluorescent aquatic tracer. Peter-Varbanets et al. (2010) observed biofouling layer thickness increased over time (ca. 200 μm) while the hydraulic resistance remained constant. It was assumed an increase of the channel's diameter (or number, Fig. 3) counteracted the effect of increased passage length due to increased biofouling layer accumulation. As the maximum axial resolution of CLSM is about 0.8 μm, the reported microscale channels must be greater than 0.8 μm and less than 3–5 μm (channels not observable under OCT). However direct and convincing visualisation of the aquatic tracer within the reported microchannel was not possible due to poor light penetration over the biofilms depth—a key limitation of CLSM in complex biofilm systems.

An alternative view is that the internal structure of a membrane biofilm is a continuous polymeric matrix (with embedded cells) with structural heterogeneity only in EPS composition and concentration, as in the conceptual model of Vrouwenvelder et al. (2017) described as the "Hair-in-Sink" effect. Therein, forced water passage occurs through a continuous network of entangled EPS chains (Fig. 8B). Permeation of water occurs through a continuous EPS mesh and exhibits preferential flow through areas of decreased polymer concentration as opposed to

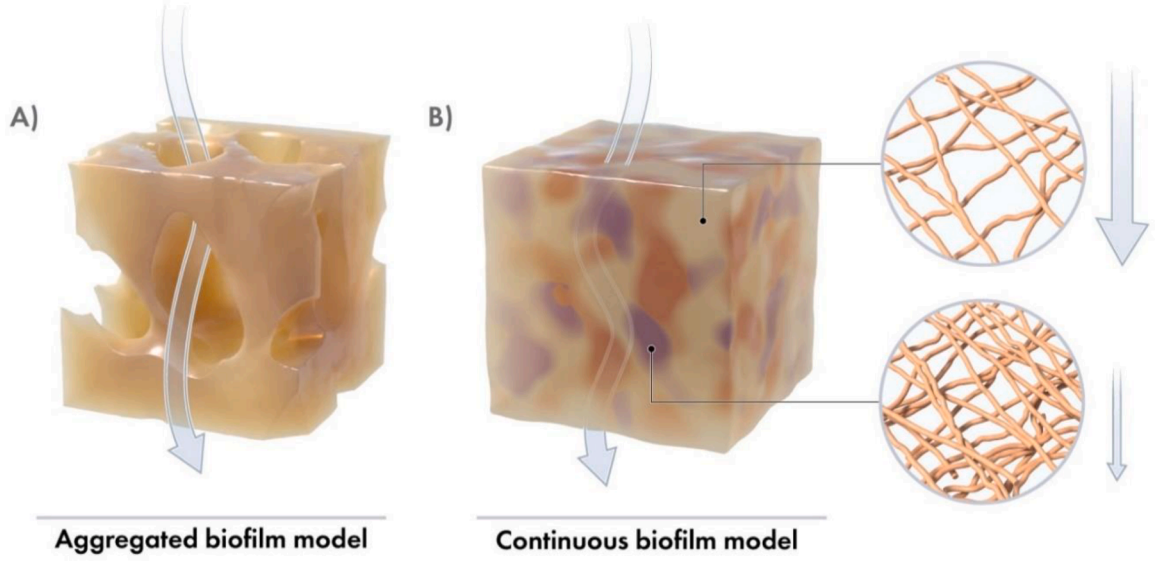

Fig. 7. Conceptual models of biofilm internal structure and conduits of permeate flow. A) Aggregated biofilm model, in which zones of absent biomass (i.e. micro or macro-pores through which water can permeate) are interspersed between areas of biomass aggregation. Hydraulic resistance is related to the square of the mean pore diameter and to the pore fraction (Fig. 3). B) Continuous biofilm model, in which permeation occurs through a continuous EPS mesh and exhibits preferential flow through areas of decreased polymer concentration as opposed to an absence of biomass. Both models are not mutually exclusive and could also occur in tandem, e.g., by a bi-pore model structure (Jafari et al., 2018; Melo 2005).

assuming the total absence of biomass (as in the micro- mesoscale channel models Melo (2005)). Hydraulic resistance is in this model imposed by areas of increased volumetric polymer concentration (i.e., decreased volume between EPS molecules) and/or passage length defined by the tortuosity within the network of entangled EPS chains (Casey 2007; Vrouwenvelder et al., 2017) (Fig. 3,7B). In such a model, the EPS entanglement is analogous to the polymeric matrix constituting the active layer of reverse osmosis membranes (Zhang et al., 2009), as opposed to the porous membranes for MF/UF. Mass transport theory in reverse osmosis membranes assumes the active layer is a non-porous structure (i.e., does not contain distinct pores) Foley (2013), in which solute and solvent molecules are dissolved and diffuse through the three-dimensional polymeric mesh (Cahill et al., 2008; Foley 2013; Libotean et al., 2008; Zhang et al., 2009). Future modelling efforts should seek to develop biofilm hydraulic models also based on the approaches describing permeate flux in reverse osmosis membranes, i.e., based on partition coefficients between EPS and the transported molecules (water, salts) and molecular diffusion. One could first assume that the partitioning coefficients are constant and uniformly distributed, but this may not be the case, given EPS are charged compounds capable of electrostatic interactions and with different hygroscopic character (Desmond et al., 2018a; Sun et al., 2020). Especially the hygroscopic properties of the EPS may be of interest to be determined and incorporated into future models.

We propose both hypothetical models from Melo (2005) and the "hair-in-sink" model from Vrouwenvelder et al. (2017) reflects the stratification observed in the physical structure of membrane biofilms. Therein the rough surface layer is representative of an aggregated biofilm structure with macro-pores, while the dense homogeneous base layer close to the membrane surface is comparable to a continuous biofilm gel (Jafari et al., 2018).

3. Can we engineer biofilms below the "pain threshold" using membrane pre-treatment and process operational controls?

The dependency of hydraulic resistance on biofilm density and its internal architecture invites efforts to reduce the hydraulic resistance by engineering internal biofilm structure. Reducing the packing density could in principle decrease the hydraulic resistance and improve filtration performance (Desmond et al., 2018c; Jafari et al., 2018). If feasible, operator intervention could focus on finding the conditions to engineer biofilm structures that allow remaining biofilms below the pain-threshold (low density and hydraulic resistance) through manipulation of feed-water composition and concentration and tailoring process operation (e.g., crossflow), rather than trying to prevent biofilm formation by imposing harsh environmental conditions.

Membrane pre-treatment and the operational crossflow velocities are design parameters that help reduce fouling and flux decline in membrane filtration systems (Akhondi et al., 2015; Howe and Clark 2006; Huck et al., 2009). Existing membrane process design focuses on reducing biofilm accumulation by restricting particle/nutrient loading and/or application of antimicrobials in hope of inhibiting bacterial growth (Beyer et al., 2017; Lee et al., 2016; Woo et al., 2015). Multiple studies and extensive industrial experience showed that biofilm mitigation is ineffective on a long term due to the biofilm adaptation to new environments. In fact, biofilm mitigation strategies could exacerbate the development of slow growing and highly resilient membrane biofilms (Vitzilaiou et al., 2019). The following section evaluates membrane pre-treatment and process operational strategies and presents parameters tailored to help engineer the formation of low-density biofilms, remaining below the pain-threshold that hampers hydraulic performance.

3.1. Feedwater quality

Nutrient concentration and, in general, raw water quality can be altered by membrane pre-treatment to lower the accumulation of in-/organic matter onto the surface of the membrane and restrict microbial growth (Griebe and Flemming 1998; Maartens et al., 2000; Vedavyasan 2007; Vrouwenvelder et al., 2010). Pre-treatment focuses on removing small, suspended particles, insoluble salts, and, more recently, nutrients (e.g., phosphorus reduction) (Vedavyasan 2007). Recent studies examining biofilm development on the surface of membrane filters with and without physical or chemical pre-treatment have shown that differences in influent composition can affect the biofilm structural development and hydraulic resistance (Javier et al., 2020a; Tang et al., 2018; Wang et al., 2008). Contrary to abiotic foulants, microorganisms can grow in the system, even if their concentration has been minimized entering the system. Microorganisms multiply on the expense of biodegradable substances, which may thus constitute the limiting factors for biofilm growth. Therefore, anything which can support microbial growth belongs to the targets to minimize when limiting biofouling.

3.1.1. Particle removal through fine sieving

Micro-sieving has been proposed to reduce the accumulation of large particles on the membrane surface, aiding performance of the Gravity-Driven Filtration (GDF). However, in GDF, Chomiak et al. (2014) demonstrated that fine particles in feed water (kaolin) induced the formation of a compact and homogeneous biofilm structure after 30 days of operation. Larger particles (diatomite) helped counterbalance the effect of fine particles due to the formation of a more heterogeneous and permeable biofilm structure. The hydraulic resistance of biofilms formed in the presence of fine particles was significantly higher than the resistance of biofilms formed in the absence of any inorganic particles or the presence of the mixed particle population. This indicates the application of conventional micro-sieving—which permits fine particle passage and large particle exclusion—could lead to the formation of a dense homogeneous biofilm structure with high hydraulic resistance. Whether improvements in flux were attributed solely to biofilm structural development or reduction in small particles forming a filter cake at the biofilm/membrane interface was not investigated. However, the overall hydraulic resistance of biofouling layers in spiral-wound MF/UF would not be likely to be reduced by the presence of larger particulate matter in the feed water.

3.1.2. Nutrient restriction and enrichment

3.2.2.1. Natural organic matter and biopolymer accumulation. Pre-treatment by granular activated carbon or slow sand-filtration can reduce loading of natural organic matter (NOM) onto the membrane surface Vedavyasan (2007). The conventional understanding of engineers is that restriction of NOM loading onto the surface of the membrane will lower adsorption of foulants onto the membrane surface and limit hydraulic resistance (Howe and Clark 2006; Huck et al., 2009; Maartens et al., 2000). However, recent evaluation by Zhang et al. (2021) evidenced the presence of a conditioning film of biopolymers on the membrane surface can drive microbial selection and engineered the formation of a thick heterogeneous biofilm with a low density (Zhang et al., 2021). It was concluded that the initial available biopolymers altered the conditions for bacterial recruitment and adhesion, and in turn influenced biofilm composition, physical structure and filtration performance. This points to the importance of cultivating initial conditioning films as a means to engineer biofilms below the threshold of interface, which are otherwise removed by conventional pre-treatment strategies. However, the selection of a pre-treatment strategy (e.g., GAC, SSF) must balance the transmission of beneficial compounds for low density biofilm development against unwanted foulants which may lead to unwanted pore-block and increased filtration resistance (e.g., humic acids).

3.2.2.2. Dissolved organic nutrients. Pre-treatment strategies are additionally used to lower the loading of dissolved organic nutrients in influent water through the membrane by applying adsorbents (e.g.,

granular activated carbon) or sand filters (Flemming et al., 1996; Griebe and Flemming 1998). It is generally anticipated lower nutrient load onto the surface of a membrane filter will lower the rate of microbial growth and biofilm establishment. In extensively pre-treated water, phosphate (P) limitation was proposed by Vrouwenvelder et al. (2010) as a method to control biofouling of spiral-wound RO membranes. The RO installation was characterized by a low feed channel pressure drop increase and low biomass concentrations in membrane elements. This installation contrasted with installations fed with less extensively pre-treated feed water (i.e., higher phosphate concentrations) and experienced a high-pressure drop increase and high biomass concentrations in first stage membranes. Membrane fouling simulator (MFS) studies by Vrouwenvelder et al. (2010) showed that low phosphate concentrations (~0.3 μg P/L) in the feed water restricted the pressure drop increase and biomass accumulation, even at high substrate (organic carbon) concentrations. Contrary reports were later provided by Desmond et al. (2018a) albeit in gravity driven ultrafiltration membranes, demonstrating membrane biofilms cultivated by excluding P addition in synthetic surface waters exhibited increased EPS production and hydraulic resistance compared to biofilms cultivated with a balanced nutrient ratio. The increase in EPS production consisted of anionic extracellular polymeric substances, which formed dense physical structures, and thereof elevated hydraulic resistance. Javier et al. (2020a) later demonstrated that biofouling control in reverse osmosis membrane systems by phosphorus limitation strongly depends on the assimilable organic carbon concentration (AOC). P restriction under non-limiting concentrations led to similar increased EPS production as described by Desmond et al. (2018a). Despite being observed in different membrane types (RO vs. ultrafiltration membranes), under different modes of operation (crossflow vs. dead-end) and likely different microbial communities, resulting biofilms demonstrated a conserved metabolic response to the imposed nutrient regime. It can be concluded that engineering heterogeneous biofilm structures with low density and hydraulic conditions is thus favoured with low concentrations of AOC and in conjunction with P limitation in both RO and UF membrane systems with and without application of hydraulic crossflow.

3.1.3. Microbial enrichment through eukaryote cultivation

Derlon et al. (2012) demonstrated that the presence of eukaryotic organisms in gravity driven ultrafiltration (GDF) systems resulted in the gradual formation of spatially heterogeneous biofilm structures with a lower hydraulic resistance. The absence of predation by metazoan organisms, resulted in flat and compact biofilm structures (Derlon et al., 2013). A practical strategy to supplement the presence of higher organism biofilm predators on the membrane surface was not provided. Tang et al. (2018) later investigated the influence of an integrated granular activated carbon (GAC)-membrane hybrid system to serve as eukaryotic "pre-incubator". Inclusion of GAC before GDF systems increased concentration of higher organisms within the membrane biofilm, improved eukaryotic predation and speculatively helped engineer more permeable and heterogeneous biofilm physical structures (Tang et al., 2018). Experimental controls were however not provided to uncouple the effects of decreased nutrient loading due to physical sorption/biological removal from effects of predation on biofilm development. The findings of Tang et al. (2018) demonstrate the early potential of a nature-based solution for the cultivation of biofilm predators to engineer the physical structure of membrane biofilms.. If so, the conventional application of antimicrobials for mitigating microbial growth would have catastrophic effects on the survival of eukaryotic organisms required for maintaining spatially heterogeneous structures with a lower hydraulic resistance.

Avoiding application of antimicrobials to maintain favourable conditions for eukaryotic predation must be balanced with the need to limit biofilm overgrowth. The following section discusses how membrane process operation conditions such transmembrane pressure and shear stress can be applied to change the EPS composition and physical structure to help maintain biofilm growth "below the pain-threshold" and sustain a low hydraulic resistance.

3.2. Membrane process operation

3.2.1. Transmembrane pressure and permeate flux

During filtration at constant permeate flux, as the biofilm accumulates on the surface of the membrane, and/or as pore blockage occurs, the transmembrane pressure must increase relative to the increase in hydraulic resistance in order to maintain contain permeate flux (Valladares Linares et al. 2015). Dreszer et al. (2014) demonstrated an increase in permeate flux due to increased TMP caused a decrease in biofilm thickness and an increase in biofilm resistance, indicating biofilm compaction. After elevated flux operation, the biofilm thickness was reduced to 75%, and the hydraulic resistance increased to 116% of the original values. OCT imaging of the biofilm with increased permeate flux revealed that the biofilm became compacted (Dreszer et al., 2014). Biofilm compression following an increase in permeate flux in response to sudden changes in TMP was also confirmed by the experiments of Desmond et al. (2018c).

In the context of engineering biofilm structure by regulation of permeate flux, consideration must be given to limiting flux (Field et al., 2011). Limiting is defined as the maximum stationary permeation flux which can be reached when increasing trans-membrane pressure. Limiting flux theory was largely developed for filtration of inert particle suspensions. Limiting flux is also observed in systems operating with membrane biofilms. During Gravity Driven filtration, stepwise increases in transmembrane pressure leads to the onset of limiting flux, but is non-ideal due to irreversible compression of the membrane biofilm (Desmond et al., 2018c). Operation below the limiting flux avoids over-compaction of the biofilm and engineers biofilm with a low hydraulic resistance. Derlon et al. (2016) indicate the selection of a lower initial flux limited compaction of the biofilm, allowing the hydraulic resistance remained low and stable over time. Meanwhile, long-term operation at an elevated transmembrane pressure/permeate flux led to reduced permeability that was attributed to a compacted biofilm. The elevated hydraulic resistance could not be attributed to increased foulant accumulation alone, and strong correlation was made to the internal structure of the biofilm. Thus, operating filtration systems below the limiting-flux offers a valid strategy to engineer biofilms with low density and thereof, hydraulic resistance.

In submersed membrane bioreactors, TMP relaxation was evaluated as a strategy to detach the membrane biofilm and allow permeate water recovery (Shi et al., 2020). However, recent investigations demonstrated poor efficacy in decreasing hydraulic resistance by TMP relaxation (Fortunato et al., 2020; Shi et al., 2020). Fortunato et al. (2020) monitored the impact of TMP relaxation in GDF systems on the physical structure of membrane biofilm. It was demonstrated that relaxation led to an increase in thickness and a decrease in the biomass specific hydraulic resistance. Obviously, the biofilm responded like a compressible sponge. No enhancement in membrane performance was reported. These results are comparable to Shi et al. (2020) who demonstrated TMP relaxation allows partial decompression of the membrane and partial detachment from the membrane. The biofilm, however, remained anchored at discrete locations across the surface of the membrane.

Decompression of the biofilm can reduce specific hydraulic resistance and density, but not enough to improve membrane performance due to the irreversible biofilm compression. Mechanical properties of membrane biofilms thus include not only an elastic (reversible) component, but also a plastic (irreversible) element (Jafari et al., 2018). Thus, to fully avoid compression of membrane biofilms and avoid the irreversible formation of dense biofilm structures, membrane modules must be operated at low and constant TMP/permeate flux to help maintain low density biofilms with high permeability.

3.2.2. Shear stress: crossflow and air scouring

Shear stress is used in membrane filtration systems applied during drinking water treatment to limit biofilm accumulation and aid the detachment of organic and inorganic material from the surface of the membrane and is cited as a biofilm mitigation strategy (Nguyen et al., 2012). However, long term application of shear stress to control biofilm development in membrane filtration seems to be unsuccessful (Dreszer et al., 2014). This could largely be due to the fact the microorganisms, unlike inert particles, can adapt their physiology to thrive in harsh hydromechanical environments and can develop resilience to imposed shear stress by increase production of highly-adhesive EPS (Park et al., 2011). Recent investigations into the impact of hydraulic shear stress induced by crossflow on biofilm development in membrane fouling simulators in drinking water applications indicate that the shear stress can actively influence the composition and physical structure of the biofilms with consequences for hydraulic resistance and filtration performance (Dreszer et al., 2014; Tang et al., 2016). Dreszer et al. (2014) investigated the influence of hydraulic regimes and concluded that operation at high crossflow velocities increased biomass accumulation and secretion of polysaccharide-rich EPS, yielding dense biofilm structures. Biomass accumulation was related to the nutrient load, which is the result of both nutrient concentration and linear flow velocity. It was demonstrated that reducing the nutrient concentration in the feed water enabled the application of higher crossflow velocities without overproduction of polysaccharide-based EPS, thus lowering the propensity to form dense homogeneous structures (Dreszer et al., 2014). This indicates the utility of combining different process control strategies (e.g., pre-treatment (particle reduction) + crossflow velocity) to engineer the chemical composition of the biopolymers, with an impact on biofilm structural development and hydraulic resistances.

The formation of dense physical structures with high hydraulic resistance under shear induced by increased crossflow velocities is comparable to the development of biofilm structures under shear induced by air scouring. Ding et al. (2016) demonstrated that the thickness of the membrane biofilms formed in gravity driven ultrafiltration membrane bioreactors operated with air scouring was lower than the thickness resulted in reactors operated without air scouring (ca. 129 vs. 344 μm). Biofilms exposed to frequent air scouring were reported to be thinner, denser and have a higher hydraulic resistance. Dreszer et al. (2014) also found that the dense biofilms contained substantially higher concentration of polysaccharides compared to biofilms formed without aeration shear. Thus, operating at lower shear stress can help develop a biofilm with lower density and lower hydraulic resistance through manipulation of EPS composition, an architectonic determinant of microbial biofilms.

From these studies it can be concluded that variable levels of shear stress induced by hydraulic crossflow and/or air scouring can be used as a process operation tool to bias formation of certain biofilm structures. Although in the short term the high shear removes part of the biofilm, operating a low shear stress (i.e. low crossflow rate) could help on the longer term to engineer global biofilm structural and hydraulic properties with lower densities and less hydraulic resistance, by avoiding compaction via tangential flow and reducing concentration of polysaccharide-based EPS compared to biofilms formed under high shear stress/crossflow environments. Application of low shear stress would first have to consider operational practicalities such as particulate concentration and required pre-treatment strategy for their reduction. Decreased shear-stress increases risk of particulate accumulation which would otherwise cause membrane clogging in the lumen of hollow-fibre membranes or feed spacer-fouling in spiral wound membrane configurations.

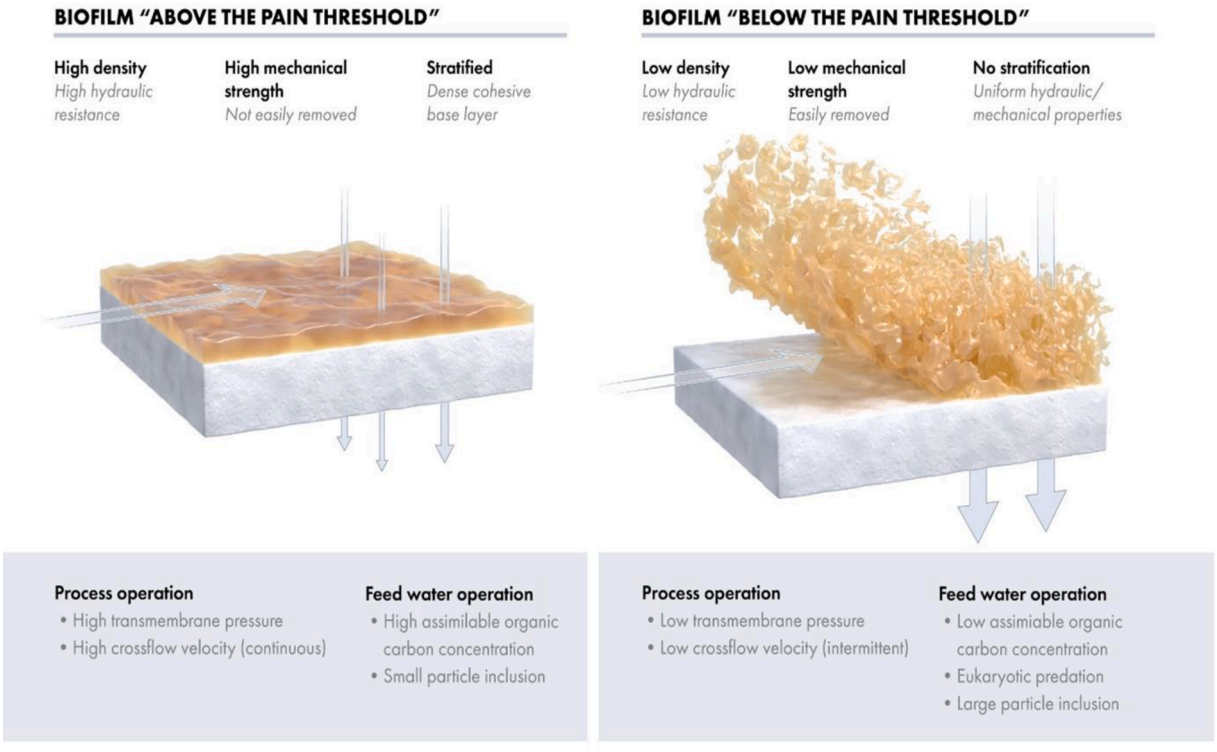

Fig. 8. Physical structure of biofilms above and below the pain-threshold in membrane filtration systems: Process operation and feed water quality can lead to biofilms effective both above and below the pain thresh-hold. Biofilms below the pain threshold (with low density and hydraulic resistance) can be engineered under conditions of low assimilable organic carbon concentration and a process operation defined by a constant TMP/permeate flux. Biofilms above the pain threshold occur under conditions of high AOC concentration and a process operation defined by increasing TMP (leading to biofilm compaction) and with high continuous crossflow velocities (leading to thin and dense biofilms). Image is a graphical representation of reviewed studies in Section 3 which report variation on biofilm physical structure in response to alternation in feedwater quality and/or process operation (Desmond et al., 2018a, Desmond et al. 2021, Desmond et al., 2018c, Jafari et al., 2018, Javier et al., 2020a, Javier et al., 2020b).

4. Future research directions

4.1. Biofilm porosity and magnetic resonance techniques

We suggest here that the quantitative reports of internal porosity in membrane biofilms are currently not supported by adequate experimental evidence nor by a reliable methodology. This is due to the recognised technical limitations of "gold standard" biofilm visualisation methods such OCT and CLSM relating to internal shadowing (OCT), compositionally dependant refractive index (OCT) and selective staining (CLSM) (Wagner and Horn 2017; Wagner et al., 2010). Future efforts should focus on incorporating established methods applied in clinical and biomedical sciences to visualise organic cellular-based structures and local fluid flow pattern. An example would be the wider use of magnetic resonance imaging (MRI) and related techniques. To date, such techniques have largely been used to simply identify the location of biofilm accumulation in a variety of support structures, relying on differences in NMR relaxation properties or self-diffusivity to realise the required image contrast between biofilm and surrounding free fluid. Future work should focus on more quantitative imaging of biofilms such that local water concentrations and thus biofilm structural heterogeneity can be determined. Whilst the resolution of such imaging is comparatively limited at present, MRI measurements can be complemented by spatially unresolved NMR measurements of self-diffusivity, which can be interpreted to determine domains of free water within the biofilm structure at the micron length-scale. However, MRI is limited by a low resolution between 30 and 50 μm and the likely occurrence of visual artefacts (e.g., shadowing) which may reduce its utility for visualising biofilm pore structures reported in numerical models by Jafari et al. (2019) to be lower than 5 μm in diameter. In terms of convective transport through biofilm structures, similar NMR techniques can be used to determine displacement probability distributions (known as propagators) inside biofilm structures and how these evolve with observation time (Manz et al., 2003; Vogt et al., 2013). This evolution is directly related to the heterogeneity of the biofilm structure and presents a uniquely powerful technique to interrogate water permeability in such structures.

4.2. How does EPS chemical composition influence hydraulic resistance of membrane biofilms?

Different EPS components can interact with inorganic ions, influencing the hydraulic resistance of membrane biofilms by biofilm structuration through intermolecular interaction (Desmond et al., 2018a; Pfaff et al., 2021). Biofilms with high concentrations of anionic EPS such as certain classes of polysaccharides (e.g., alginate-like exopolysaccharide) and eDNA can form dense biofilm structures with high hydraulic resistance (Desmond et al., 2018a). However, whether alginate layers are a suitable surrogate system to mirror complex physiology of polymicrobial biofilms (e.g., spatiotemporal variation in local composition and hydraulics) is subject to critical debate and requires clarification. Observations made in alginate gel-layers must be validated in polymicrobial biofilm systems to determine the relevance of experimental observations. Furthermore, the influence of local physico-chemical characteristics such as local pH on the EPS material properties (e.g., viscoelasticity and plasticity) and, consequently, on permeability is less known. It is anticipated the physicochemical characteristics of EPS can determine the biofilms overall hygroscopic character and influence the partitioning coefficient between external water and that present in the biofilm structure. It has been claimed that hydrophilic EPS would decrease the partitioning coefficient between water and EPS, increasing the permeability by decreasing biofilm hydraulic resistance (Sun et al., 2020). Conversely, hydrophobic components of EPS, would increase the partitioning coefficient of water into the biofilm, therein increasing over all hydraulic resistance. Recent developments in-situ biofilm analysis have opened the possibility to link local flow velocities within an intact biofilm structure to local EPS compositions over the biofilm depth. The combined use of computational fluid dynamics and MRI/NMR to determine local flow distribution (Pintelon et al., 2009) and 2–3D confocal Raman microscopy to determine local chemical compositions of EPS (Desmond et al., 2018a) may assist in co-localisation of permeability values with specific compositions of EPS in biofilm structures. This would improve understanding of how variation in local EPS compositions can influence local and overall hydraulic resistance of membrane biofilms.

4.3. Why are membrane biofilms stratified?

Membrane biofilms with a stratified structure were reported by Jafari et al. (2018) and Jafari et al. (2019) on gravity driven ultrafiltration membranes. The stratified biofilm exhibited a rough surface layer above a dense base layer which had high hydraulic resistance and adhesion to the membrane surface. How and why stratified biofilm structures occur is the subject of debate with several hypotheses put forward. One hypothesis suggests that the formation of a dense base layer is due to the nutrient limitation (possibly, both electron donor and acceptor) at the membrane surface in co-diffusional biofilms (Alpkvist et al., 2006). In biofilms formed on membranes, not only co-diffusion of electron acceptor and donor takes place, but also convection through the permeate flux aiding rapid assimilation of nutrient. As such, the permeate of GDF systems have a low concentration of assimilable organic carbon (AOC) that can restrict microbial growth (<80 μg AOC/L) (Chomiak et al., 2015). Low nutrient limiting conditions at the biofilm/membrane interface may lead to activation of the bacterial stringent stress response (local "starvation"), which triggers local secretion of extracellular polymeric substrates (EPS) at the biofilms base, increasing local density and therein hydraulic resistance (Alpkvist et al., 2006; Jafari et al., 2018; Picioreanu et al., 2000). Alternatively, the base layer may be constituted by the accumulation of dead-cell mass that could be not researched by nutrient diffusion. However, whether the low nutrient concentrations at the biofilm-membrane interface are sufficient to increase EPS secretion and lead to the formation of a stratified biofilm structure is not known and requires detailed investigation.

5. Conclusions

When investigated under different experimental conditions (e.g., compression, feedwater variation), hydraulic resistance depends more on biofilm density than on any other biofilm structure parameter (e.g., thickness, surface roughness) or resistance parameter (pore-blocking, membrane resistance). We conclude efforts to reduce overall filtration resistance should focus on reducing the density of membrane biofilms. Reducing the density of membrane biofilms can be achieved by modulating biofilm growth via pre-treatment and operational processes, such as (i) feed water nutrient composition/concentration, (ii) transmembrane pressure (TMP) and (iii) cross-flow velocity (CFV), alone or in tandem. Consideration must be given to whether laboratory studies linking pre-treatment and process operational conditions to low density biofilm formation are scalable to application and whether the concept of "biofilm engineering" can be extended to other biofilm parameters such as mechanical stability to enable better management of recalcitrant biofilms in water engineering systems (e.g., pipelines and/or, cooling towers).

1. Hydraulic resistance of membrane biofilms deviates from assumptions derived from classic particle-based filtration theory as biofilms (being made by living organisms, unlike inert particle layers) can adjust their physical and chemical properties in adaptation to operationally defined environmental conditions. This invites greater opportunity for regulation of biofilm hydraulic resistance by

manipulation of growth conditions by pre-treatment or process operation.

2. Hydraulic resistance has greater dependency on the density of biofilm EPS. EPS density, and thereof biofilm density, is governed by intermolecular interactions and local hydromechanical forces. High concentrations of polysaccharides and eDNA serve as ligands for divalent cations, which by decreasing the volume between EPS strands lead to biofilm structures with low permeability. However greater consideration must be given to experimental systems for biofilm development to ensure fidelity to "real-life" conditions and avoid system-based artefacts (e.g., narrow selection of EPS, low microbial diversity)
3. Pre-treatment of membrane influent can help engineer biofilms with low density and hydraulic resistance through manipulation of biopolymer loading and nutrient ratio of dissolved organic nutrient. Feedwater with low assimilable organic carbon concentration combined with phosphorus limitation in membrane filtration systems help forming biofilms with lower concentrations of polysaccharide and eDNA and lower propensity to self-assemble into dense structures with high hydraulic resistance. Promotion of eukaryotic predation on the membrane surface can assist formation of more permeable biofilm structures.
4. Operating MF/UF membrane modules with low shear stress induced by hydraulic flow or gas sparging helps reducing mechanical compression of the biofilm structure, thus lowering the hydraulic resistance of the biofilm. The friction force exerted by the viscous permeate flow compresses the biofilm material, thereby reducing the pore size and limiting the water passage.

Declaration of Competing Interest

The authors declare that they have no known competing financial interests or personal relationships that could have appeared to influence the work reported in this paper.

Acknowledgements

The authors would like to highlight the contribution of Xavier Pita, Scientific Illustrator at the King Abdullah University of Science and Technology (KAUST) for production of the Fig. 5, 6, 8, 9.

The research reported in this publication was supported by funding from King Abdullah University of Science and Technology (KAUST) and RWTH-Aachen University (2020).

References

Akhondi, E., Wu, B., Sun, S., Marxer, B., Lim, W., Gu, J., Liu, L., Burkhardt, M., McDougald, D., Pronk, W., 2015. Gravity-driven membrane filtration as pretreatment for seawater reverse osmosis: linking biofouling layer morphology with flux stabilization. Water Res. 70, 158–173.

Alpkvist, E., Picioreanu, C., van Loosdrecht, M.C., Heyden, A., 2006. Three-dimensional biofilm model with individual cells and continuum EPS matrix. Biotechnol. Bioeng. 94 (5), 961–979.

Beyer, F., Laurinonyte, J., Zwijnenburg, A., Stams, A.J., Plugge, C.M., 2017. Membrane fouling and chemical cleaning in three full-scale reverse osmosis plants producing demineralized water. J. Eng. 2017.

Bucs, S.S., Linares, R.V., Marston, J.O., Radu, A.I., Vrouwenvelder, J.S., Picioreanu, C., 2015. Experimental and numerical characterization of the water flow in spacer-filled channels of spiral-wound membranes. Water Res. 87, 299–310.

Cahill, D.G., Freger, V., Kwak, S.-.Y., 2008. Microscopy and microanalysis of reverse-osmosis and nanofiltration membranes. MRS Bull. 33 (1), 27–32.

Casey, E., 2007. Tracer measurements reveal experimental evidence of biofilm consolidation. Biotechnol. Bioeng. 98 (4), 913–918.

Chomiak, A., Sinnet, B., Derlon, N., Morgenroth, E., 2014. Inorganic particles increase biofilm heterogeneity and enhance permeate flux. Water Res. 64, 177–186.

Chomiak, A., Traber, J., Morgenroth, E., Derlon, N., 2015. Biofilm increases permeate quality by organic carbon degradation in low pressure ultrafiltration. Water Res. 85, 512–520.

Coussy, O., 2004. Poromechanics. John Wiley & Sons.

Derlon, N., Grütter, A., Brandenberger, F., Sutter, A., Kuhlicke, U., Neu, T.R., Morgenroth, E., 2016. The composition and compression of biofilms developed on ultrafiltration membranes determine hydraulic biofilm resistance. Water Res. 102, 63–72.

Derlon, N., Koch, N., Eugster, B., Posch, T., Pernthaler, J., Pronk, W., Morgenroth, E., 2013. Activity of metazoa governs biofilm structure formation and enhances permeate flux during gravity-driven membrane (GDM) filtration. Water Res. 47 (6), 2085–2095.

Derlon, N., Peter-Varbanets, M., Scheidegger, A., Pronk, W., Morgenroth, E., 2012. Predation influences the structure of biofilm developed on ultrafiltration membranes. Water Res. 46 (10), 3323–3333.

Desmond, P., Best, J.P., Morgenroth, E., Derlon, N., 2018a. Linking composition of extracellular polymeric substances (EPS) to the physical structure and hydraulic resistance of membrane biofilms. Water Res. 132, 211–221.

Desmond, P., Böni, L., Fischer, P., Morgenroth, E., Derlon, N., 2018b. Stratification in the physical structure and cohesion of membrane biofilms—Implications for hydraulic resistance. J. Memb. Sci. 564, 897–904.

Desmond, P., Morgenroth, E., Derlon, N., 2018c. Physical structure determines compression of membrane biofilms during gravity driven membrane (GDM) ultrafiltration. Water Res. 143, 539–549.

Ding, A., Liang, H., Li, G., Derlon, N., Szivak, I., Morgenroth, E., Pronk, W., 2016. Impact of aeration shear stress on permeate flux and fouling layer properties in a low pressure membrane bioreactor for the treatment of grey water. J Memb Sci 510, 382–390.

Dreszer, C., Flemming, H.C., Zwijnenburg, A., Kruithof, J.C., Vrouwenvelder, J.S., 2014. Impact of biofilm accumulation on transmembrane and feed channel pressure drop: effects of crossflow velocity, feed spacer and biodegradable nutrient. Water Res. 50, 200–211.

Dreszer, C., Vrouwenvelder, J.S., Paulitsch-Fuchs, A.H., Zwijnenburg, A., Kruithof, J.C., Flemming, H.C., 2013. Hydraulic resistance of biofilms. J Memb Sci 429 (0), 436–447.

Field, R.W., Pearce, G.K.J.A.i.c. and science, i. (2011) Critical, sustainable and threshold fluxes for membrane filtration with water industry applications. 164(1–2), 38–44.

Flemming, H.-.C., 2020. Biofouling and me: My Stockholm Syndrome With Biofilms, 173. Water Research, 115576.

Flemming, H.-.C., Baveye, P., Neu, T.R., Stoodley, P., Szewzyk, U., Wingender, J., Wuertz, S., 2021. Who put the film in biofilm? The migration of a term from wastewater engineering to medicine and beyond. NPJ Biofilms Microbiomes 7 (1), 10.

Flemming, H.-.C., Griebe, T., Schaule, G., 1996. Antifouling strategies in technical systems—A short review. Water Sci. Technol. 34 (5–6), 517–524.

Foley, G., 2013. Membrane Filtration: a Problem Solving Approach with MATLAB. Cambridge University Press.

Fortunato, L., Jeong, S., Wang, Y., Behzad, A.R., Leiknes, T., 2016. Integrated approach to characterize fouling on a flat sheet membrane gravity driven submerged membrane bioreactor. Bioresour. Technol. 222, 335–343.

Fortunato, L., Lamprea, A.F., Leiknes, T., 2020. Evaluation of membrane fouling mitigation strategies in an algal membrane photobioreactor (AMPBR) treating secondary wastewater effluent. Sci. Total Environ. 708, 134548.

Fortunato, L., Qamar, A., Wang, Y., Jeong, S., Leiknes, T., 2017. In-situ assessment of biofilm formation in submerged membrane system using optical coherence tomography and computational fluid dynamics. J. Memb. Sci. 521, 84–94.

Giraudier, S., Hellio, D., Djabourov, M., Larreta-Garde, V., 2004. Influence of weak and covalent bonds on formation and hydrolysis of gelatin networks. Biomacromolecules 5 (5), 1662–1666.

Griebe, T., Flemming, H.-.C., 1998. Biocide-free antifouling strategy to protect RO membranes from biofouling. Desalination 118 (1–3), 153-IN159.

Heistad, A., Scott, T., Skaarer, A., Seidu, R., Hanssen, J., Stenström, T., Stenström, T., Stenström, T.J.W.S. and Technology (2009) Virus removal by unsaturated wastewater filtration: effects of biofilm accumulation and hydrophobicity. 60(2), 399–407.

Herzberg, M., Elimelech, M., 2007. Biofouling of reverse osmosis membranes: role of biofilm-enhanced osmotic pressure. J. Memb. Sci. 295 (1–2), 11–20.

Herzberg, M., Kang, S., Elimelech, M.J.E.s. and technology (2009) Role of extracellular polymeric substances (EPS) in biofouling of reverse osmosis membranes. 43(12), 4393–4398.

Howe, K.J., Clark, M.M., 2006. Effect of coagulation pretreatment on membrane filtration performance. American Water Works Assoc. 98 (4), 133–146.

Huck, P.M., Peldszus, S., Haberkamp, J., Jekel, M., 2009. Assessing the performance of biological filtration as pretreatment to low pressure membranes for drinking water. Environ. Sci. Technol. 43 (10), 3878–3884.

Jafari, M., D'haese, A., Zlopasa, J., Cornelissen, E., Vrouwenvelder, J.S., Verbeken, K., Verliefde, A., van Loosdrecht, M., Picioreanu, C., 2020. A comparison between chemical cleaning efficiency in lab-scale and full-scale reverse osmosis membranes: role of extracellular polymeric substances (EPS). J. Memb. Sci. 609, 118189.

Jafari, M., Derlon, N., Desmond, P., van Loosdrecht, M.C., Morgenroth, E., Picioreanu, C., 2019. Biofilm compressibility in ultrafiltration: a relation between biofilm morphology, mechanics and hydraulic resistance. Water Res. 157, 335–345.

Jafari, M., Desmond, P., van Loosdrecht, M.C., Derlon, N., Morgenroth, E., Picioreanu, C., 2018. Effect of biofilm structural deformation on hydraulic resistance during ultrafiltration: a numerical and experimental study. Water Res. 145, 375–387.

Javier, L., Farhat, N.M., Desmond, P., Linares, R.V., Bucs, S., Kruithof, J.C., Vrouwenvelder, J.S., 2020a. Biofouling control by phosphorus limitation strongly depends on the assimilable organic carbon concentration. Water Res. 183, 116051.

Javier, L., Farhat, N.M., Vrouwenvelder, J.S., 2020b. Enhanced hydraulic cleanability of biofilms developed under a low phosphorus concentration in reverse osmosis membrane systems. Water Res. X, 100085.

Jermann, D., Pronk, W., Meylan, S. and Boller, M.J.W.r. (2007) Interplay of different NOM fouling mechanisms during ultrafiltration for drinking water production. 41 (8), 1713–1722.
Lee, E.-J., An, A.K., Hadi, P., Yan, D.Y., Kim, H.-S., 2016. A mechanistic study of in situ chemical cleaning-in-place for a PTFE flat sheet membrane: fouling mitigation and membrane characterization. Biofouling 32 (3), 301–312.
Libotean, D., Giralt, J., Rallo, R., Cohen, Y., Giralt, F., Ridgway, H.F., Rodriguez, G., Phipps, D, 2008. Organic compounds passage through RO membranes. J. Memb. Sci. 313 (1–2), 23–43.
Maartens, A., Swart, P., Jacobs, E., 2000. Membrane pretreatment: a method for reducing fouling by natural organic matter. J. Colloid Interface Sci. 221 (2), 137–142.
Manz, B., Volke, F., Goll, D., Horn, H.J.B., 2003. Measuring local flow velocities and biofilm structure in biofilm systems with magnetic resonance imaging (MRI), 84 (4), 424–432.
Martin, K., Bolster, D., Derlon, N., Morgenroth, E., Nerenberg, R., 2014. Effect of fouling layer spatial distribution on permeate flux: a theoretical and experimental study. J. Memb. Sci. 471, 130–137.
Mayer, C., Moritz, R., Kirschner, C., Borchard, W., Maibaum, R., Wingender, J., Flemming, H.-.C., 1999. The role of intermolecular interactions: studies on model systems for bacterial biofilms. Int. J. Biol. Macromol. 26 (1), 3–16.
McDonogh, R., Schaule, G., Flemming, H.-.C., 1994. The permeability of biofouling layers on membranes. J. Memb. Sci. 87 (1–2), 199–217.
Melo, L., 2005. Biofilm physical structure, internal diffusivity and tortuosity. Water Sci. Technol. 52 (7), 77–84.
Nguyen, T., Roddick, F., Fan, L., 2012. Biofouling of water treatment membranes: a review of the underlying causes, monitoring techniques and control measures. Membranes 2 (4), 804–840.
Park, A., Jeong, H.-.H., Lee, J., Kim, K.P., Lee, C.-.S., 2011. Effect of shear stress on the formation of bacterial biofilm in a microfluidic channel. Biochip J 5 (3), 236.
Peter-Varbanets, M., Hammes, F., Vital, M., Pronk, W., 2010. Stabilization of flux during dead-end ultra-low pressure ultrafiltration. Water Res. 44 (12), 3607–3616.
Peter-Varbanets, M., Margot, J., Traber, J., Pronk, W., 2011. Mechanisms of membrane fouling during ultra-low pressure ultrafiltration. J Memb Sci 377 (1), 42–53.
Peter-Varbanets, M., Zurbrügg, C., Swartz, C., Pronk, W., 2009. Decentralized systems for potable water and the potential of membrane technology. Water Res. 43 (2), 245–265.
Pfaff, N.-.M., Kleijn, J.M., van Loosdrecht, M.C., Kemperman, A.J., 2021. Formation and ripening of alginate-like exopolymer gel layers during and after membrane filtration. Water Res., 116959
Picioreanu, C., Van Loosdrecht, M.C., Heijnen, J.J., 2000. Effect of diffusive and convective substrate transport on biofilm structure formation: a two-dimensional modeling study. Biotechnol. Bioeng. 69 (5), 504–515.
Pintelon, T., Graf von der Schulenburg, D., Johns, M, 2009. Towards optimum permeability reduction in porous media using biofilm growth simulations. Biotechnol. Bioeng. 103 (4), 767–779.
Radu, A., Vrouwenvelder, J., Van Loosdrecht, M., Picioreanu, C., 2010. Modeling the effect of biofilm formation on reverse osmosis performance: flux, feed channel pressure drop and solute passage. J. Memb. Sci. 365 (1–2), 1–15.
Radu, A.I., Vrouwenvelder, J.S., van Loosdrecht, M.C., Picioreanu, C., 2012. Effect of flow velocity, substrate concentration and hydraulic cleaning on biofouling of reverse osmosis feed channels. Chem. Eng. J. 188, 30–39.
Seader, J.D., Henley, E.J., Roper, D.K., 1998. Separation Process Principles. wiley New York, Chapter 14.
Shi, D., Liu, Y., Fu, W., Li, J., Fang, Z., Shao, S., 2020. A combination of membrane relaxation and shear stress significantly improve the flux of gravity-driven membrane system. Water Res., 115694
Siebdrath, N., Farhat, N., Ding, W., Kruithof, J., Vrouwenvelder, J.S., 2019. Impact of membrane biofouling in the sequential development of performance indicators: feed channel pressure drop, permeability, and salt rejection. J Memb Sci 585, 199–207.
Sun, X., Wang, L., Fu, R., Yang, Y., Cheng, R., Li, J., Wang, S., Zhang, J., 2020. The chemical properties and hygroscopic activity of the exopolysaccharide lubcan from Paenibacillus sp. ZX1905. Int. J. Biol. Macromole. 164, 2641–2650.
Tang, X., Ding, A., Qu, F., Jia, R., Chang, H., Cheng, X., Liu, B., Li, G., Liang, H., 2016. Effect of operation parameters on the flux stabilization of gravity-driven membrane (GDM) filtration system for decentralized water supply. Environ. Sci. Pollut. Res. 1–10.
Tang, X., Pronk, W., Ding, A., Cheng, X., Wang, J., Xie, B., Li, G., Liang, H., 2018. Coupling GAC to ultra-low-pressure filtration to modify the biofouling layer and bio-community: flux enhancement and water quality improvement. Chem. Eng. J. 333, 289–299.
Valladares Linares, R., Wexler, A., Bucs, S.S., Dreszer, C., Zwijnenburg, A., Flemming, H.-.C., Kruithof, J., Vrouwenvelder, J., 2015. Compaction and relaxation of biofilms. Desalination Water Treat 57 (28), 12902–12914.
Vedavyasan, C., 2007. Pretreatment trends—An overview. Desalination 203 (1–3), 296–299.
Vitzilaiou, E., Stoica, I.M., Knøchel, S., 2019. Microbial biofilm communities on reverse osmosis membranes in whey water processing before and after cleaning. J. Memb. Sci. 587, 117174.
Vogt, S.J., Sanderlin, A.B., Seymour, J.D., Codd, S.L.J.B., 2013. Permeability of a growing biofilm in a porous media fluid flow analyzed by magnetic resonance displacement-relaxation correlations, 110 (5), 1366–1375.
Vrouwenvelder, H., Dreszer, C., Linares, R.V., Kruithof, J.C., Mayer, C. and Flemming, H.-.C. (2017) The Perfect Slime: Microbial extracellular Polymeric Substances. Flemming, H.-C., Neu, T.R. and Wingender, J. (eds), pp. 193–206, IWA Press, London.
Vrouwenvelder, H., Van Paassen, J., Folmer, H., Hofman, J.A., Nederlof, M., Van der Kooij, D, 1998. Biofouling of membranes for drinking water production. Desalination 118 (1), 157–166.
Vrouwenvelder, J.S., Beyer, F., Dahmani, K., Hasan, N., Galjaard, G., Kruithof, J.C., Van Loosdrecht, M.C.M., 2010. Phosphate limitation to control biofouling. Water Res. 44 (11), 3454–3466.
Wagner, M., Horn, H., 2017. Optical coherence tomography in biofilm research: a comprehensive review. Biotechnol. Bioeng. 114 (7), 1386–1402.
Wagner, M., Taherzadeh, D., Haisch, C., Horn, H., 2010. Investigation of the mesoscale structure and volumetric features of biofilms using optical coherence tomography. Biotechnol. Bioeng. 107 (5), 844–853.
Wang, L., Wang, X., Fukushi, K.-i., 2008. Effects of operational conditions on ultrafiltration membrane fouling. Desalination 229 (1–3), 181–191.
Woo, Y.C., Lee, J.J., Tijing, L.D., Shon, H.K., Yao, M., Kim, H.-.S., 2015. Characteristics of membrane fouling by consecutive chemical cleaning in pressurized ultrafiltration as pre-treatment of seawater desalination. Desalination 369, 51–61.
Zhang, L., Graham, N., Derlon, N., Tang, Y., Siddique, M.S., Xu, L. and Yu, W.J.J.o.M.S. (2021) Biofouling by ultra-low pressure filtration of surface water: The paramount role of initial available biopolymers. 640, 119740.
Zhang, X., Cahill, D.G., Coronell, O., Mariñas, B.J., 2009. Absorption of water in the active layer of reverse osmosis membranes. J. Memb. Sci. 331 (1–2), 143–151.